

CookieBox White Paper

Averell Gatton

December 18, 2018

Abstract

This document summarizes back of the envelope calculations and SIMION simulations defining the design space of the Cookie Box. We analyze linear time of flight spectrometers as well as hemispherical analyzers.

1 Mission

The CookieBox will provide angle and energy information of streaked photo-electrons sufficient for ptychographic reconstruction of the SASE substructure of one and two color pulses from the LCLS-II. This information must be provided with as high a rep-rate as possible.

2 Constraints

2.1 Space Constraints

The CookieBox must fit into the beamline layout of the TMO hutch. The beamline is bounded by the floor, $1.2m$ below the beamline, and by the adjacent SXR beamline which is approximately a meter away horizontally in the plane containing the beam propagation directions of both beamlines. Free space exists above and to one side of the CookieBox. Space permits for the radial length to be as large as $1m$. In the propagation direction, space is much more limited, and the design should be as compact as possible. More information is needed on the space constraints in this direction.

However, size is limited by the functionality of the TMO space. The machine itself will be removed and replaced at points, and a maximally sized machine of $\simeq 2m$ diameter will be unwieldy.

The FEE CookieBox must fit in a more constrained space. The maximum radial extent is $.6$ meters.

2.2 Angular Streaking Reconstruction Constraints

In order to reconstruct the FEL SASE substructure, the CookieBox must resolve electrons to $.25eV$ over a $100eV$ window with angular information over 360

degrees. Reconstruction is still robust with angular bins as large as 22.5° (16 bins).

The photoelectrons to be streaked are born with a $\cos^2[\theta]$ distribution and with a presumed energy of 330eV . The electrons are streaked by 50eV and fall in the energy range $E_i = [280, 380]$.

Additionally, the 1MHz rate of the FEL imposes a maximum flight time of approximately $1\mu\text{s}$. While this can be extended by the length of the shortest flight time of electrons born in the previous bunch, this is not advisable as there is potential for crosstalk between shots.

2.3 FEL Duty Cycle Constraints

The FEL will operate at 1MHz which equates to a bunchspacing of $1\mu\text{s}$. All electrons in each eToF must be cleared between each bunch, which fixes the maximum drift time as the bunchspacing time. The maximum transit time in the drift tube, neglecting the initial free flight and deceleration region (which is a small time in comparison for high energy electrons) is plotted in figure 1. The x-axis in figure 1 begins at $.1\text{eV}$ and even these low energy electrons manage to travel drift in less than one microsecond. Therefore, a very small offset voltage on the second deceleration mesh, sufficient to increase the energy past $.1\text{eV}$ for all electrons that pass the deceleration region, will insure that all electrons clear the flight tube between shots.

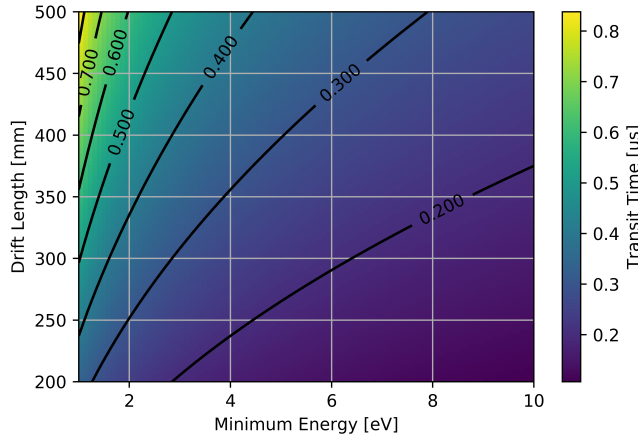


Figure 1: Maximum transit time in the drift tube as a function of energy and drift tube length.

3 Time of Flight (ToF) Analysis

The traditional CookieBox design has been a radial array of 16 ToF electron energy analyzers. These function by decelerating and focusing the electrons into a drift tube where they are eventually collected by an MCP. In this way time of flight is mapped to energy. Specifying the initial energy as E and retarded energy as E_{ret} , the initial free drift as r_o , the decelerating length as d_a , the time spent in region r_o and d_a as t_a , the deceleration as a , the time in the drift tube as t_d , and the drift tube distance as d_d , we can write:

$$t_a + t_d = \frac{r_o}{\sqrt{2E/m}} + \frac{2 * d_a}{\sqrt{2E/m} + \sqrt{2E_{ret}/m}} + \frac{d_d}{\sqrt{2E_{ret}/m}}. \quad (1)$$

If we assume that the deceleration, a , is large, then we can drop the t_a terms as a first approximation:

$$t_d = \frac{d_d}{\sqrt{2E/m}}, \quad (2)$$

and solve for E in terms of t_d

$$E = \frac{m * d_d^2}{2t_d^2}. \quad (3)$$

Now we assume there is some small error so that $t_d = t - \Delta t$ such that:

$$E = \frac{m * d_d^2}{2t^2} \frac{1}{(1 - \Delta t/t)^2}. \quad (4)$$

Taylor expansion keeping only the first term gives

$$E = \frac{m * d_d^2}{2t^2} (1 + 2\Delta t/t) = E_o (1 + 2\Delta t/t). \quad (5)$$

The error in energy is then

$$\Delta E = E_o * (2\Delta t/t). \quad (6)$$

This immediately yields a minimum length of the ToF design if the maximum upper bound of Δt is known. Setting this upper bound is the subject of the next subsection.

3.1 Time Uncertainty

There are three primary contributions to the time uncertainty in the ToF; the spatial extent of the photoionization, the difference in path length for equal energy electrons (electrostatic lens dispersion), and the response time of the MCP/anode readout. For argument, let us assume a flight tube of 500mm through which an electron of 100eV will travel in approximately 100ns.

To begin with, we can confidently say that $50ps$ of time uncertainty in the MCP/anode readout can be achieved by the use of digitizers and peak processing. It should be noted that the anode readout spread as quoted by the manufacturer is $450ps$ and the timing resolution is dependent on our ability to extract peak positions from the pile-up signal.

The spatial extent of the photoionization is determined by the position of the focus and by the original energy of the photoelectrons. When the CookieBox is in dedicated use, we expect less than $10\mu m$ spot size. Assuming $280eV$ photoelectrons to find the maximum transit time of the focus, we find a $1ps$ transit time. Therefore, for small foci we can safely neglect the error from ionization volume. Conversely, when the CookieBox is used for pulse characterization in service to another experiment, we expect the focus size to be on the order of $1mm$. With $280eV$ photoelectrons this translates to $100ps$.

The time dispersion of mono-energetic electrons is somewhat hard to estimate and depends upon the initial angular acceptance and lens systems. In the ideal scenario with no lensing or magnetic field distortions, the path length to a flat MCP (assuming curved mesh components for optimal fields) is modified by $\Delta d = \sin(\theta)R_{mcp}$, where R_{mcp} is the radius of the MCP. The energy error can again be calculated starting from

$$t_d = \frac{d_d + \Delta d}{\sqrt{2E/m}} \quad (7)$$

and ending with

$$\Delta E = E * (2\Delta d/d_d) = E * (2R_{mcp}^2/d_d^2), \quad (8)$$

with the assumption $\sin(\theta) = R_{mcp}/d_d$. The path length difference for a $d = 500mm$ and $R_{mcp} = 12.5mm$ is $310\mu m$ corresponding to an error of $E*6.25e^{-4}$. For $100eV$ photoelectrons $310\mu m$ path length difference translates to a time uncertainty of $50ps$.

3.2 Design Prototype

If we assume a small focus size (near zero error from photoionization), the analytical form of the energy error is

$$\Delta E = 2 * E * \sqrt{\left(\frac{R_{mcp}^2}{d_d^2}\right)^2 + \left(\frac{\Delta t_{mcp}}{t}\right)^2} \quad (9)$$

$$= 2 * E * \sqrt{\left(\frac{R_{mcp}^2}{d_d^2}\right)^2 + \frac{2E}{m_e} \left(\frac{\Delta t_{mcp}}{d_d}\right)^2}. \quad (10)$$

By inserting constants as outlined in the previous subsection ($\Delta t_{mcp} = 50ps$ and $R_{mcp} = 12.5mm$) and assuming the maximal electron energy of $100eV$, the numerical relation between energy resolution and drift length can be plotted as

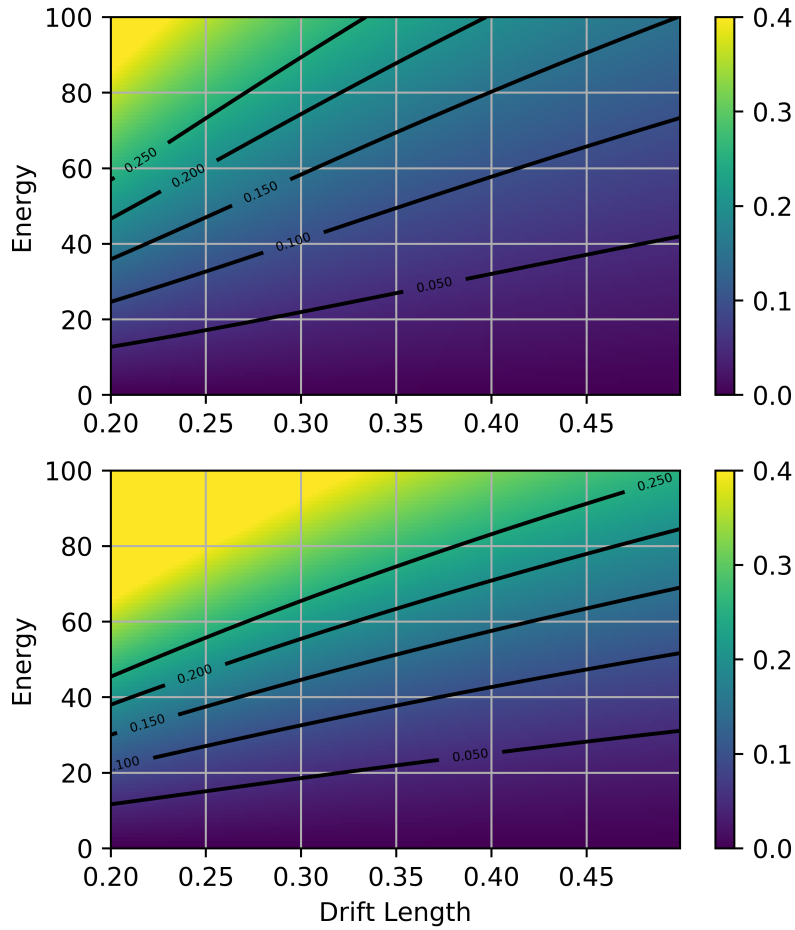


Figure 2: Energy error as a function of ToF drift lenght for 50 ps (top) and 100 ps (bottom) time error.

in figure 2. The energy resolution is shown for a 50 ps time error (top plot) and for 100 ps of time error (bottom plot).

The graphs suggest that .5m length drift regions are sufficient for achieving .25eV resolution with a time budget of 50 ps .

The collection efficiency as a function of drift tube lenght with the assumption of 87.5mm of free flight and deceleration is shown in figure 3.

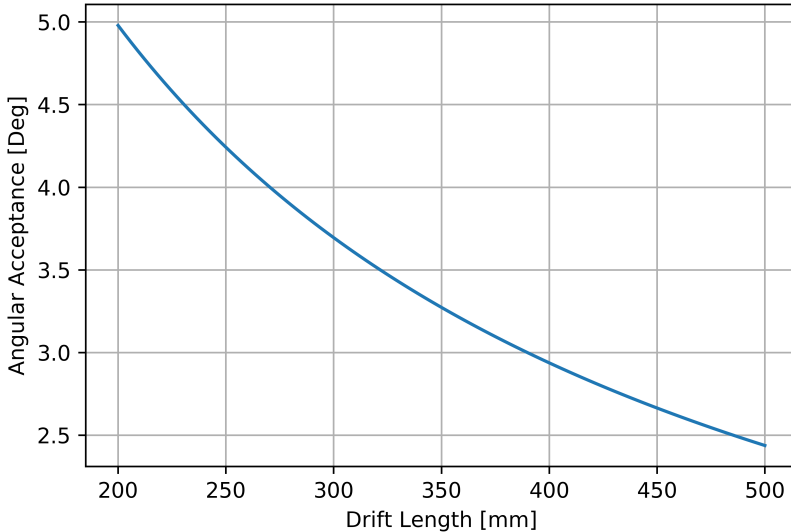


Figure 3: Angular acceptance as a function of drift tube length with a fixed free flight length of 87.5mm and a detector diameter of 25mm .

4 Focal Volume Analysis

The size of the focal volume will directly impact the energy resolution in a number of ways. Electrons born away from the ideal center of the ToF array will have travel different path lengths with different angular velocity. First we will calculate the transit time difference and then proceed to calculate the effect of small variations in angular velocity.

4.1 Transit Time

The simplest way to model the transit time difference is to assume the electrons must travel some distance on the order of the focal spot size and then divide by the electron velocity. Results of a simple calculations are shown in figure 4. For focal volumes $50\mu\text{m}$ wide, the error is about 25ps for the angular streaking case.

4.2 Angular Velocity

The worst case change in angle between two electrons of equivalent energy entering the drift region at the same starting point can be calculated directly from geometric considerations. If we fix the length to the deceleration region

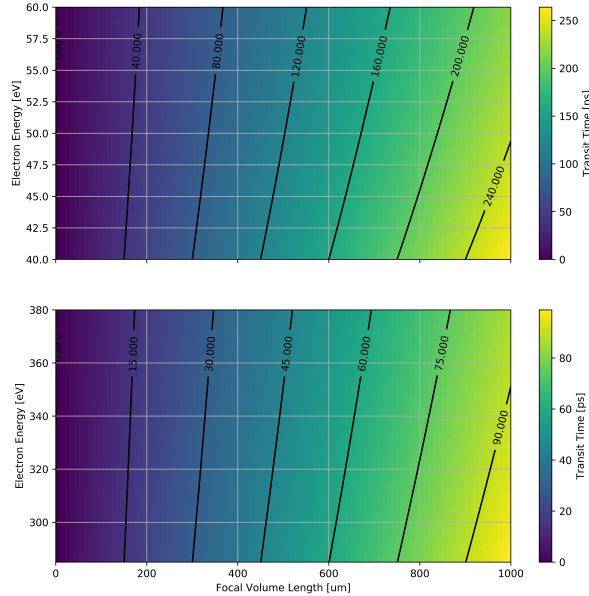


Figure 4: Focal Volume transit time as a function of energy and focal volume size.

$l_1 = 37.5\text{mm}$ and label the focal offset as f , then the angular offset is:

$$\sin(\theta) = \frac{f}{l_1}.$$

The change in energy is then:

$$\delta E = E_o * (1 - \cos(\theta))^2 = E_o * (1 - \frac{f}{l_1})^2.$$

The results for photoelectrons of around 50eV energy are shown in figure 5. Clearly, the angle error introduces minimal shifts in the energy.

Furthermore, it is seen that the translational velocity introduced is on the order of $1/1000$ of the initial velocity, which is far smaller than the natural spread in translational velocity inherent to the electron distribution flying into the spectrometer. From this we conclude that the focal volume is not 'sliced' by the long drift tube - all electrons entering the deceleration tube from the focal volume will be collected.

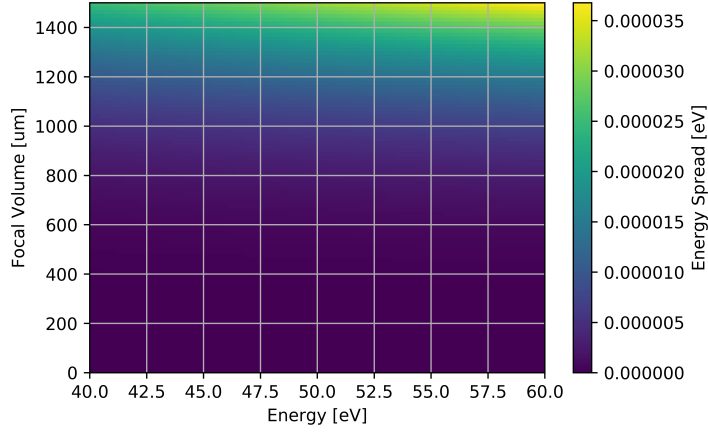


Figure 5: Energy error caused by angular offset due to focal volume size.

4.3 Focal Volume Acceptance

Each cookie will have some angular acceptance dictated by the initial opening aperture, its distance from the ionization point, and the final detector size. Naively disregarding the finite width of the opening aperture to each cookie, we can approximate the lower bound of the accepted area as

$$\frac{x}{l_1} = \frac{d_{det}}{l_2 + l_3},$$

where l_i are the initial drift (1), deceleration (2), and drift (3) lengths of the eToF, d_{det} is the detector diameter, and x is the accepted spot diameter. We can further refine this approximation by simply adding the l_1 aperture width. This results in an accepted spot diameter as shown in figure 7

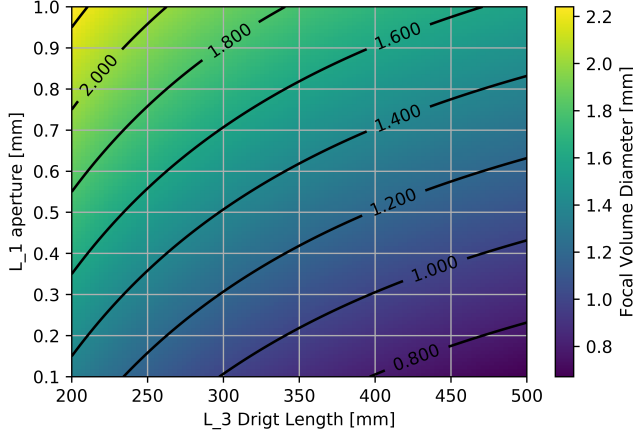


Figure 6: Diameter of the focus for a 25mm detector and $l_1 = 12.5\text{mm}$.

5 Curved Mesh

Both $1/r$ potentials and perfect flight dynamics will depend on curved mesh. Mesh introduce micro lensing and field leakage which are both dependent on the gradient of the potential on either side of the mesh. Micro-lensing requires SIMION simulations for accurate prediction of flight path deflection angle. Field leakage is an unsolved problem that cannot be simulated in SIMION for a number of reasons.

The curved mesh at the end of the drift tube will introduce differing path-lengths to the flat MCP, held at high voltage some distance away. We calculate the time uncertainty introduced from this path difference. First, we can neglect the initial electron energy as the accelerating field for the MCP will be nearly $V_{accel} = 2\text{keV}$. The time spent in transit from the curved mesh to the MCP is:

$$\begin{aligned} t &= \left(\frac{2 * d}{a} \right)^{1/2} \\ &= \left(\frac{2 * (d + \delta d)}{a} \right)^{1/2} \\ &= \sqrt{\frac{2 * d}{a}} \left(1 + \frac{2\delta d}{d} \right)^{1/2} \\ &\simeq t_o \left(1 + \frac{\delta d}{d} \right), \end{aligned}$$

where we have used a series expansion. Clearly, the time uncertainty introduced is linearly proportional to the transit time to the detector. Given a 2keV accelerating potential and a 5mm spacing, the transit time is 377ps. the maximum

pathlength difference is related to the angular acceptance (total flight length), and is

$$\delta d_{max} = r_d * \sin(\theta_{acc}),$$

where r_d is the detector radius and θ_{acc} the acceptance angle. The maximum time error introduced for a range of angular acceptances is plotted in figure ??.

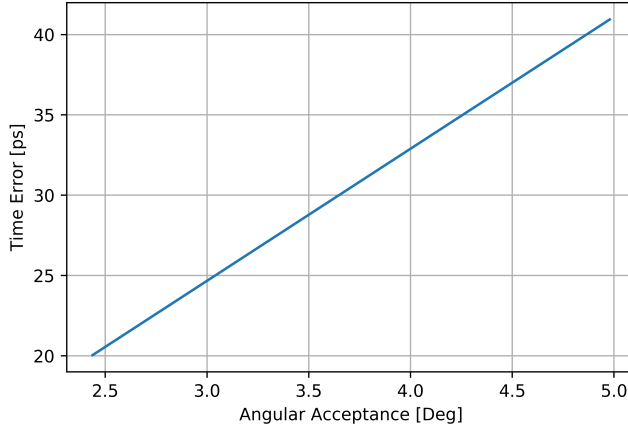


Figure 7: Error introduced by the curved mesh and flat MCP, for a spacing of 5mm and accelerating voltage of 2keV.

6 Simion Simulations

To increase collection efficiency, lens systems can be employed. Given the ratio of the energy window to total energy, chromatic aberration in the ion lens optics is severe and unavoidable. It is impossible to adequately focus electrons at the high end of the range without completely diverging electrons on the low end. Therefore, a simple lens system can only hope to focus low energy electrons. There is one workaround to this reality. After the drift tube, electrons are already separated in time and an accelerating lens system focusing onto the MCP can increase collection efficiency albeit at the expense of energy resolution.

Simulations have been conducted in SIMION to measure the energy efficiency and collection angle of a such a scheme and are shown in figure 8 for a 600mm ToF with a full radial angular collection (using a 25mm diameter detector) of 2.4° degrees. A single ToF is simulated and is constructed of an initial curved mesh followed by a flat mesh separating the deceleration region from the drift tube, and a third mesh in front of the MCP. A lensing field prior to the drift tube and the addition of the post drift collection increases the angular collection

to as large as 10 degrees. The ragged nature of the simulation data suggests that the simulation is having trouble handling some electron trajectories. The

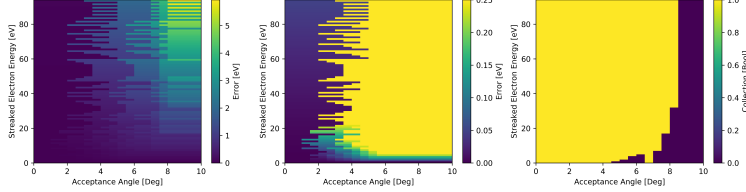


Figure 8: SION simulation results for energy error as a function of electron energy and total acceptance angle for a 600mm long ToF. Left: error for the full acceptance angle under test. Middle: same as left but the energy error has been clipped at .25eV. Right: collection boolean showing collection, 1, or a miss 0.

left most plot of figure 8 shows the full energy resolution range, which degrades to as great as 5eV at the full acceptance angle of 8° degrees. The central plot in figure 8 is the same as the left plot except for that the energy scale has been truncated at .25eV to highlight the design criteria energy resolution. The right most edge of the jagged region most probably represents the real energy resolution – better simulation and more introspection are required. The right most plot of figure 8 shows the collection boolean for electrons of particular energy and angle. High energy electrons are collected with up to 8° degrees while low energy electrons suffer from divergent lensing. The total collection efficiency of 16 ToF on a $\cos^2[\theta]$ distribution is plotted in figure 9. Collection efficiency is nearly 20% at 8°, which is more than enough to satisfy coincidence experiments.

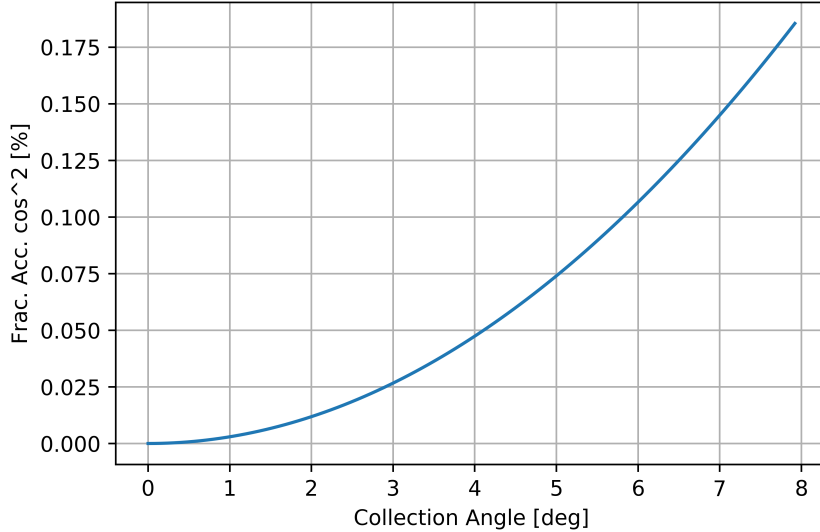


Figure 9: Collection efficiency for a 600mm long ToF assuming a \cos^2 distribution.

7 Retarding Fields

This section focuses on the best way to retard the electron velocity without limiting collection efficiency or introducing error.

7.1 Ideal Potential

Generally speaking, the retardation potential in the cookie box should not introduce any lensing effect. The spherically symmetric potential is determined from the Laplace equation:

$$\Delta f = \frac{1}{\rho} \frac{\partial}{\partial \rho} \left(\rho^2 \frac{\partial f}{\partial \rho} \right) + \frac{1}{\rho^2 \sin(\theta)} \frac{\partial}{\partial \theta} \left(\sin(\theta) \frac{\partial f}{\partial \theta} \right) + \frac{1}{\rho^2 \sin^2(\theta)} \frac{\partial^2 f}{\partial \phi^2} = 0. \quad (11)$$

The general form for the solution in spherical coordinates is:

$$f = (Ar^l + Br^{-(l+1)})Y_{lm}(\theta, \phi), \quad (12)$$

with Y_{lm} the spherical harmonic of order lm . Since we demand no angular dependence, we must set $l = m = 0$. This leaves:

$$f = Ar + Br^{-1}, \quad (13)$$

from which we can immediately set $A = 0$ as the field must be zero at infinity. Finally

$$f = Br^{-1}, \quad (14)$$

and we conclude that the ideal potential must be inversely proportional to r .

The question now is how to produce a $1/r$ potential in the spectrometer for a variety of different voltages. The equation for the potential and its boundary conditions are given as:

$$\begin{aligned} V(r) &= \kappa/r + C \\ V(r_o) &= 0 \\ V(r_f) &= V_f. \end{aligned}$$

With the constants:

$$\begin{aligned} \kappa &= \frac{r_f r_o}{r_f - r_o} V_f \\ C &= -\frac{r_f}{r_f - r_o} V_f. \end{aligned}$$

The final form of the potential is:

$$V(r) = V_f \left(\frac{\frac{r_f r_o}{r_f - r_o} \frac{1}{r}}{r} - \frac{r_f}{r_f - r_o} \right).$$

If we divide by the total constant current across the part, then we get a function for the total resistance between r_o and r :

$$R(r) = R_{tot} \left(\frac{\frac{r_f r_o}{r_f - r_o} \frac{1}{r}}{r} - \frac{r_f}{r_f - r_o} \right).$$

From this it is clear that the shape of the resistance does not change after scaling the voltage as long as the total resistance is kept constant.

7.2 Razor-blades

Discrete plates can be used to define potential similar to those used in COLTRIMS and VMI spectrometers. Given that the deceleration regions should be as short as possible, the size of these elements is extremely small. Total width available for 16, 32, and 64 cookies as a function of radius is shown in figure 10. Since the razor blades must be twice as wide as they are separated radially, the design quickly becomes cramped. Additionally, the more razor blades the better, up to the point where a stack of razorblades can be used with peek tape as insulator between them. Finally, the blades must be connected in series with accurate resistors. These could be hard to source at the correct resistance to meet the $1/r$ potential.

Fundamentally, the razor blades will introduce a discrete step nature to the potential. While the physics of the poisson equation will average these steps

out in the center of the deceleration region, electrons that fly close to the razors will be perturbed, degrading resolution. A more ideal solution is to have a perfectly varying potential on the walls of the deceleration tube, as discussed in the next section.

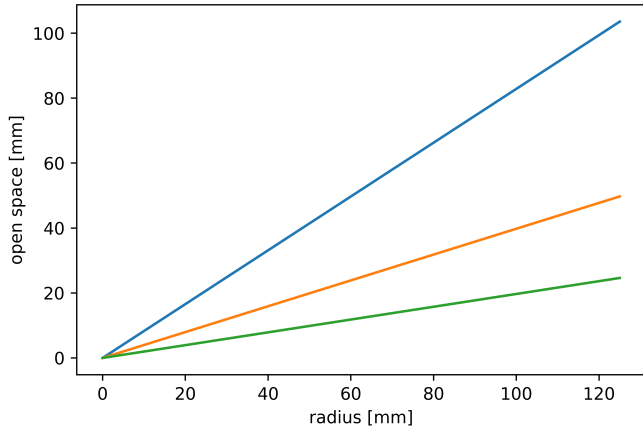


Figure 10: Open space in the azimuthal direction, cookie plane, as a function of radius for 16 (blue), 32 (orange), and 64 (green) cookies.

7.3 Silicon Carbide

A semiconductor of constant resistance can be made to have a perfectly scaled $1/r$ potential on its surface by suitable choice of cross-sectional area. Silicon Carbide has been identified as an ideal semiconductor material that can be machined and powder sintered with high accuracy into arbitrary shapes. The resistance of the final product can vary from $1 - 1e7\Omega$. First we derive the functional shape of the area of the SiC part. Then, assuming a resistance of $1e5$, the calculations for the cross section of a radially expanding tube are recorded.

7.4 Derivation of area function

With ρ the resistivity of the chosen material at any point is:

$$dV(r) = IR(r) = \frac{I\rho}{A(r)} dr.$$

The potential drop in a material with a constant current is:

$$\begin{aligned}\int_{r_o}^r dV &= \int_{r_o}^r IR(r') \\ V(r) - V(r_o) &= \int_{r_o}^r \frac{I \rho}{A(r')} dr'.\end{aligned}$$

The boundary conditions are:

$$\begin{aligned}V(r_o) &= 0 \\ V(r_f) &= V_f.\end{aligned}$$

We desire

$$\begin{aligned}V(r) &= \kappa/r + C \\ \kappa/r + C &= \int_{r_o}^r \frac{I \rho}{A(r')} dr',\end{aligned}$$

with κ and C constants with values according to the above boundary conditions:

$$\begin{aligned}\kappa &= \frac{r_f r_o}{r_f - r_o} V_f \\ C &= -\frac{r_f}{r_f - r_o} V_f.\end{aligned}$$

Taking the derivative:

$$\begin{aligned}\frac{\partial}{\partial r} (\kappa/r + C) &= \frac{\partial}{\partial r} \left(\int_{r_o}^r \frac{I \rho}{A(r')} dr' \right) \\ -\kappa/r^2 &= \frac{\partial}{\partial r} \left(\int_{r_o}^r \frac{I \rho}{A(r')} dr' \right)\end{aligned}$$

To solve this equation we can guess that $A(r) = \gamma r^2$. The above equation becomes

$$\begin{aligned}-\frac{\kappa}{r^2} &= \frac{I \rho}{\gamma r^2} \\ \gamma &= \frac{I \rho}{\kappa} \\ &= -\frac{I}{V_f} \rho \frac{r_f - r_o}{r_f r_o} \\ &= -\frac{\rho}{R_{tot}} \frac{r_f - r_o}{r_f r_o},\end{aligned}$$

Where we have combined $V_f/I = R_{tot}$ as the total resistance across the part. Immediately, the available parameters become the start radius r_o , the stop radius r_f , the part resistivity ρ , and the total desired resistivity across the part R_{tot} , which dictates the the total current. Clearly the shape of the resistance does not change with changing voltage, only with changing total resistance, resistivity, or radial start and stop points.

7.5 SiC Part Design

We choose an an expanding hollow cylindrical cone as the geometry and solve for the thickness of the cone as a function of radius. The equations for area of an expanding hollow cone with inner radius x_i and outer radius x_o :

$$A(r) = \pi(x_o^2 - x_i^2).$$

$$\gamma r^2 = \pi(x_o^2 - x_i^2).$$

Let us assume that the inner and outer radii of the cylinder expand according to

$$x_i = mr + c \quad (15)$$

$$x_o = x_i + d(r), \quad (16)$$

where m is the slope determined by the space constraints of a cookie, $d(r)$ is the thickness of the cylinder as a function of radial distance from the ionization point, and c is the initial thickness of the cylinder at r_o . The equation for area becomes:

$$\kappa r^2 = \pi((x_i^2 + 2x_i d(r) + d^2(r)) - x_i^2). \quad (17)$$

$$0 = -(\gamma/\pi)r^2 + 2(mr + c)d(r) + d^2(r). \quad (18)$$

The thickness can be found with the quadratic equation using constants q:

$$q_a = 1 \quad (19)$$

$$q_b = 2(mr + c) \quad (20)$$

$$q_c = -\frac{\gamma r^2}{\pi} \quad (21)$$

$$(22)$$

Calculations for an example part with parameters, $V_f = -280$, $r_o = 62.5\text{mm}$, $r_f = 112.5\text{mm}$, $c = 2.5\text{mm}$, $I = 1\text{mA}$, and $R_{tot} = 280\text{k}\Omega$, are shown in figure 11. Clearly, the SiC part can be made with dimensions small enough to fit in the constraints of the cookie and yet large enough to be practical in the first place.

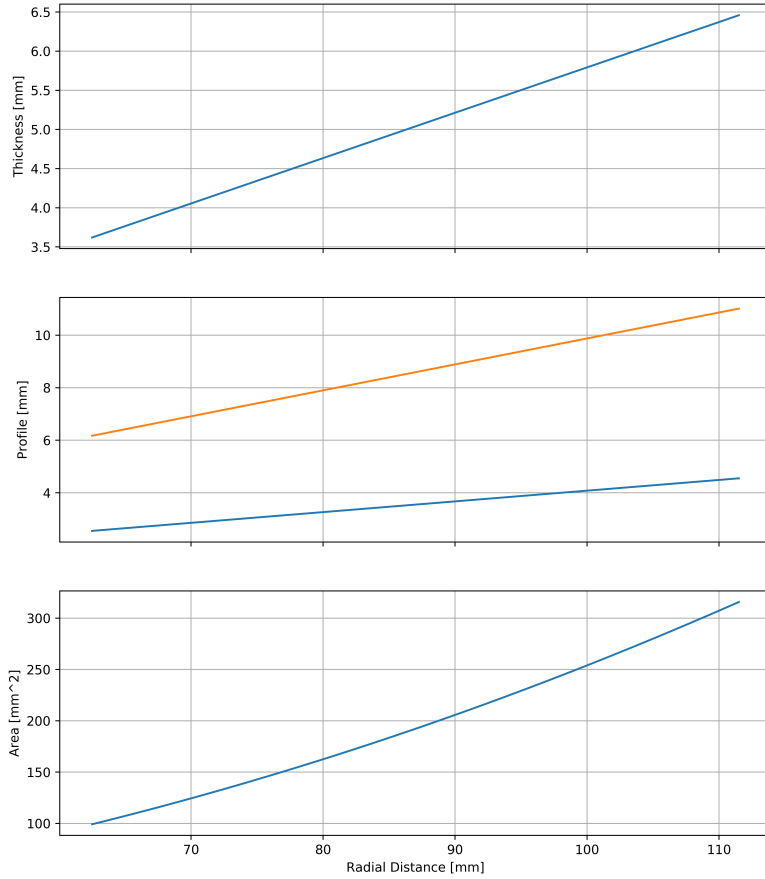


Figure 11: Geometry calculations for expanding cylinder producing a $1/r$ potential. Parameters are $V_f = -280V$, $r_o = 62.5mm$, $r_f = 112.5mm$, $c = 2.5mm$, $I = 1mA$, $R_{tot} = 280k\Omega$. Wall thickness, top. profile of a cylinder wall middle: inner wall blue, outer wall orange. Cross sectional area, bottom.

8 Multiplexing

The simulation results above demonstrate that larger collection efficiency can be obtained using lens systems while retaining good electron energy resolution for high energy electrons. With 16 spectrometers there is believed to be an

overabundance of angular information. Therefore, the spectrometers can be run with different retarding potentials to target different energy ranges of the photoelectron distribution. With such a scheme, high angular acceptance with adequate energy resolution can be made available for coincidence streaking experiments.